Monitoring statistics of the ERS-2 scatterometer for ESA

cycle 91

(Project Ref. 15988/02/I-LG)

Hans Hersbach
European Centre for Medium-Range Weather Forecasts,
Shinfield Park, Reading, RG2 9AX, England
Tel: (+44 118) 9499476, e-mail: dal@ecmwf.int

February 15, 2004

1 Introduction

On 21 August 2003, the world-wide dissemination of ERS-2 data was restarted. Due to a failure of both on-board LBR tape recorders two months earlier, only data is being received for data within the visibility range of a ground station. In practice this limits coverage to the North-Atlantic, part of the Mediterranean, the Gulf of Mexico, and to a small part of the Pacific north-west from the US and Canada (see Figure 2).

Since 8 December 2003, a new ground station became operational at West Freugh (Scotland, UK), filling the gap in data coverage over the North-Atlantic. However, at ECMWF, data for this station was only received from 23:47 UTC 15 January 2004 onwards. Its area of coverage, with the exception of the previously existing gap, is now reported by more than one ground station, which leads to a duplication in dissemination. Locations of vector wind cells between stations can differ up to 12km. The UWI winds are mostly almost identical, however, the result of the de-aliasing is occasionally not equal, resulting in anti-parallel winds. Some examples are shown in Figure 13.

The quality of the UWI product was monitored at ECMWF for cycle 91. Results were compared to those obtained from the previous cycle, as well for data received during the nominal period in 2000 (up to cycle 59).

The ERS-2 scatterometer data was not used in the 4D-Var data assimilation system at ECMWF. However, it is being processed passively in the operational suite and assimilated actively (on the basis of CMOD5) in the experimental suite that is scheduled to become operational in one month.

During cycle 91, data was received between 21:02 UTC 29 December 2003 and 20:59 UTC 2 February 2004 and for all 6-hourly batches. However, for the batches around 06 UTC 10 January 2004 only 6 observations were received, and for 06 UTC 26 January 2004 all 464 observations were rejected by the ESA quality control flag.

Mostly, the asymmetry between fore and aft incidence angles was within bounds (3 degrees). Peaks up to 7 degrees occurred for 12 UTC 10 January, 12 UTC 19 January and between 12 UTC 25 January and 00 UTC 26 January 2004. The combined k_p and yaw-error flag was set for these cases. Although there was some solar activity during cycle 91, no magnetic storms occurred around these periods of large errors in attitude.

Compared to cycle 90, the agreement with ECMWF first-guess (FGAT) fields worsened. Relative bias levels became more negative (from -0.51 m/s to -0.61 m/s), and scatter has again increased (from 1.65 m/s to 1.71 m/s). Part of this deterioration is caused by seasonal variations for the regional data set. However, the less optimal results appear to be concentrated in a relatively small area south-west of the previously existing data-void area in the North Atlantic (see Figure 3). Also, the degradation was largest in the near range, while the relative standard deviation was nearly unaltered in the far range.

The quality of both the UWI and de-aliased CMOD4 wind direction was stable.

Compared to nominal data in 2000, bias levels for both backscatter and wind speed are more optimal. Standard deviations of wind speed are less optimal to those for 2000. A fair comparison, however, cannot be made due to large differences in data coverage.

The cycle-averaged evolution of performance relative to ECMWF FGAT winds is displayed in Figure 1. Figure 2 shows global maps of the over cycle 91 averaged UWI data coverage and wind climate, Figure 3 the comparison with FGAT.

The ECMWF assimilation system was not changed during cycle 91.

2 ERS-2 statistics from 30 December 2003 to 2 February 2004

2.1 Sigma0 bias levels

The average sigma0 bias levels (compared to simulated sigma0's based on ECMWF model first-guess winds) stratified with respect to antenna beam, ascending or descending track and as function of incidence angle (i.e. across-node number) is displayed in Figure 4.

Compared to cycle 90, bias levels were nearly unchanged. The situation is slightly better than that for nominal data in 2000 (see Figure 1 of the cyclic reports for cycle 48 to 59). The dependency of the bias as function of incidence angle is small, and most negative in the near range. Internode differences are slightly smaller than for the nominal period. Bias levels are in between 0.0 and -0.5 dB.

The data volume of ascending and descending tracks are nearly equal.

2.2 Incidence angles

For ESACA, across-node binning is, like the old processor, retained on a 25km mesh. From simple geometrical arguments it follows that variations in yaw attitude will lead to asymmetries between the incidence angles of the fore and aft beam. Indeed, this has been observed. Figure 5 gives a time evolution of this asymmetry, showing rapid variations, which are typical for yaw attitude errors. Also in this figure, the occasions for which the combined k_p-yaw quality flag was set are indicated by red stars. The relation with incidence-angle asymmetries is obvious.

From Figure 5 it is seen that during cycle 91 there were three anomalous periods (10, 19 and 25 January 2004). They could not be associated with solar activity.

2.3 Distance to cone history

The distance to the cone history is shown in Figure 6. Curves are based on data that passed all QC, including the test on the k_p-yaw flag, however subject to the land and sea-ice check at ECMWF (see cyclic report 88 for details).

Time series are very (due to lack of statistics) noisy, especially for the first nodes. This makes it difficult to identify peaks that might indicate a low data quality. Most spikes are a result from low data volumes. The volatile behavior on 25 January 2004 arises from the rejection of almost all data by the combined k_p-yaw flag (see also Figure 5).

Compared to cycle 90, average levels have decreased from 1.23 to 1.17 and are now about 7% higher than for nominal data (see top panel Figure 1).

2.4 UWI minus First-Guess wind history

In Figure 7, the UWI minus ECMWF first-guess wind-speed history is plotted.

The history plot shows many peaks. Similar results apply for the history of de-aliased CMOD4 winds versus FGAT (Figure 9). Most peaks are a result of low data volume. Others indicate a real discrepancy between UWI and ECMWF winds.

An example (top panel of Figure 12) is shown for 00:55 UTC 17 January for data in the area of low performance as discussed in the introduction (the red area in the lower panel of Figure 3). In the near-range of the displayed swath the UWI winds do not look realistic, are much weaker than the FGAT winds, and in addition suffer from de-aliasing problems.

Another example is given in the lower panel of Figure 12. Here the large difference with the FGAT winds arise from a relative displacement of a front. So for this case the UWI winds do look realistic.

Average bias levels and standard deviations of UWI winds relative to FGAT winds are displayed in Table 1. From this it is seen that the bias of both the UWI and CMOD4 product have become more negative by 0.1 m/s. Internode differences are comparable, being most negative in the near range (see also third panel of Figure 1). The average bias level is still better than for nominal data in 2000 (UWI: -0.61 m/s now, was -0.79 m/s for cycle 59).

	cycle 90		cycle 91	
	UWI	CMOD4	UWI	CMOD4
speed STDV	1.65	1.63	1.71	1.70
node 1-2	1.63	1.58	1.78	1.73
node 3-4	1.56	1.54	1.66	1.65
node 5-7	1.56	1.56	1.64	1.63
node 8-10	1.60	1.59	1.68	1.67
node 11-14	1.61	1.61	1.70	1.70
node 15-19	1.68	1.68	1.69	1.69
speed BIAS	-0.51	-0.49	-0.61	-0.59
node 1-2	-1.21	-1.16	-1.25	-1.20
node 3-4	-0.89	-0.81	-0.93	-0.86
node 5-7	-0.56	-0.52	-0.64	-0.61
node 8-10	-0.32	-0.31	-0.44	-0.43
node 11-14	-0.28	-0.28	-0.38	-0.37
node 15-19	-0.24	-0.23	-0.39	-0.39
direction STDV	29.3	19.8	28.9	19.6
direction BIAS	-3.3	-2.9	-2.8	-2.9

Table 1: Biases and standard deviation of ERS-2 versus ECMWF FGAT winds in m/s for speed and degrees for direction

The standard deviation of UWI winds compared to cycle 90 has worsened as well (1.71 m/s, was 1.65 m/s). The increase is largest in the near range (0.15 m/s) and only 0.01 m/s at the highest nodes. This reverses the internode dependency completely; performance is now worst in the near range, instead of in the far range for cycle 90.

Figure 11 displays the locations for which UWI winds were more than 8 m/s weaker (top panel) and more than 8 m/s stronger (lower panel) than FGAT winds. Far lower winds cluster in the area south west of the previously existing data gap, where now the same observations are reported by two ground stations. The case of the top panel of Figure 12 is an example. Occasionally the de-aliasing algorithm results in a different solution between the stations. Two examples are given in Figure 13.

The distribution of far stronger UWI winds is slightly more homogeneous. The case displayed in the lower panel of Figure 12 represents an example.

For cycle 91 the (UWI - model) direction standard deviations were ranging between 20 and 40 degrees (Figure 8). Sharp peaks are the result of low data volumes. For de-aliased CMOD4 winds values between 20 and 30 degrees are most common (Figure 10). With respect to cycle 90, the average standard deviation (see Table 1) of the UWI wind direction was slightly lower (28.9 degrees, was 29.3 degrees). The same applies for de-aliased CMOD4 winds (19.6 degrees, was 19.8 degrees). Bias levels in wind direction were also very similar (-3.3 degrees, was -2.3 degrees for UWI; -2.9 degrees unaltered for CMOD4).

2.5 Scatterplots

Scatterplots of model 10 m first-guess winds versus ERS-2 winds are displayed in Figures 14 to 17. Values of standard deviations and biases are slightly different from those displayed in Table 1. Reason for this is that, for plotting purposes, the in 0.5 m/s resolution ERS-2 winds have been slightly perturbed (increases scatter with 0.02 m/s), and that zero wind-speed ERS-2 winds have been excluded (decreases scatter with about 0.05 m/s).

The scatterplot of UWI wind speed versus FGAT (Figure 14) is very similar to that for (at ECMWF inverted) de-aliased CMOD4 winds (Figure 16). It confirms that the ESACA inversion scheme is working properly. The enhanced standard deviation with respect to cycle 90 (1.72 m/s, was 1.61 m/s), seems to arise from slightly more collocations between low UWI and strong FGAT winds.

Winds derived on the basis of CMOD5 are displayed in Figure 15. The bias compared to FGAT winds remains small for all wind domains (on average -0.01 m/s, was 0.06 m/s) The relative standard deviation is lower than for CMOD4 winds (1.69 m/s versus 1.72 m/s).

Figure Captions

Figure 1: Evolution of the performance of the ERS-2 scatterometer averaged over 5-weekly cycles from 12 December 2001 (cycle 69) to 2 February 2004 (end cycle 91) for the UWI product (solid, star) and de-aliased winds based on CMOD4 (dashed, diamond). Results are based on data that passed the UWI QC flags. For cycle 85 two values are plotted; the first value for the global set, the second one for the regional set. Dotted lines represent values for cycle 59 (5 December 2000 to 17 January 2001), i.e. the last stable cycle of the nominal period. From top to bottom panel are shown the normalized distance to the cone (CMOD4 only) the standard deviation of the wind speed compared to FGAT winds, the corresponding bias (for UWI winds the extreme inter-node averages are shown as well), and the standard deviation of wind direction compared to FGAT.

Figure 2: Average number of observations per 12H and per 125km grid box (top panel) and wind-climate (lower panel) for UWI winds that passed the UWI flags QC and a check on the collocated ECMWF land and sea-ice mask.

Figure 3: The same as Figure 2, but now for the relative bias (top panel) and standard deviation (lower panel) with ECMWF first-guess winds.

Figure 4: Ratio of $< \sigma_0^{0.625} > / < \mathrm{CMOD4(FirstGuess)}^{0.625} >$ converted in dB for the fore beam (solid line), mid beam (dashed line) and aft beam (dotted line), as a function of incidence angle for descending and ascending tracks. The thin lines indicate the error bars on the estimated mean. First-guess winds are based on the in time closest (+3h, +6h, +9h, or +12h) T511 forecast field, and are bilinearly interpolated in space.

Figure 5: Time series of the difference in incidence angle between the fore and aft beam. Red stars indicate the occurrences for which the combined k_p-yaw flag

was set.

Figure 6: Mean normalized distance to the cone computed every 6 hours for nodes 1-2, 3-4, 5-7, 8-10, 11-14 and 15-19 (solid curve close to 1 when no instrumental problems are present). The dotted curve shows the number of incoming triplets in logarithmic scale (1 corresponds to 60,000 triplets) and the dashed one indicates the fraction of complete (based on the land-sea mask at ECMWF) sea-located triplets rejected by ESA flags, or by the wind inversion algorithm (0: all data kept, 1: no data kept).

Figure 7: Mean (solid line) and standard deviation (dashed line) of the wind speed difference UWI - first guess for the data retained by the quality control.

Figure 8: Same as Fig. 7, but for the wind direction difference. Statistics are computed only for wind speeds higher than 4 m/s.

Figures 9 and 10: Same as Fig. 7 and 8 respectively, but for the de-aliased CMOD4 data.

Figure 11: Locations of data during cycle 91 for which UWI winds are more than 8 m/s weaker (top panel) respectively stronger (lower panel) than FGAT, and on which QC on UWI flags and the ECMWF land/sea-ice mask was applied.

Figure 12: Comparison between UWI (red) and ECMWF FGAT (blue) winds for a case on 17 January 2004 (top panel) respectively 12 January (lower panel).

Figure 13: Two situations for which the de-aliasing software resulted in different solutions between two stations reporting the same data point.

Figure 14: Two-dimensional histogram of first guess and UWI wind speeds, for the data kept by the UWI flags, and QC based on the ECMWF ice and land-sea mask. Circles denote the mean values in the y-direction, and squares those in the x-direction.

Figure 15: Same as Fig. 14, but for wind direction. Only wind speeds higher than 4m/s are taken into account.

Figure 16: Same as Fig. 14, but for de-aliased CMOD4 winds.

Figure 17: Same as Fig. 14, but for de-aliased CMOD5 winds.

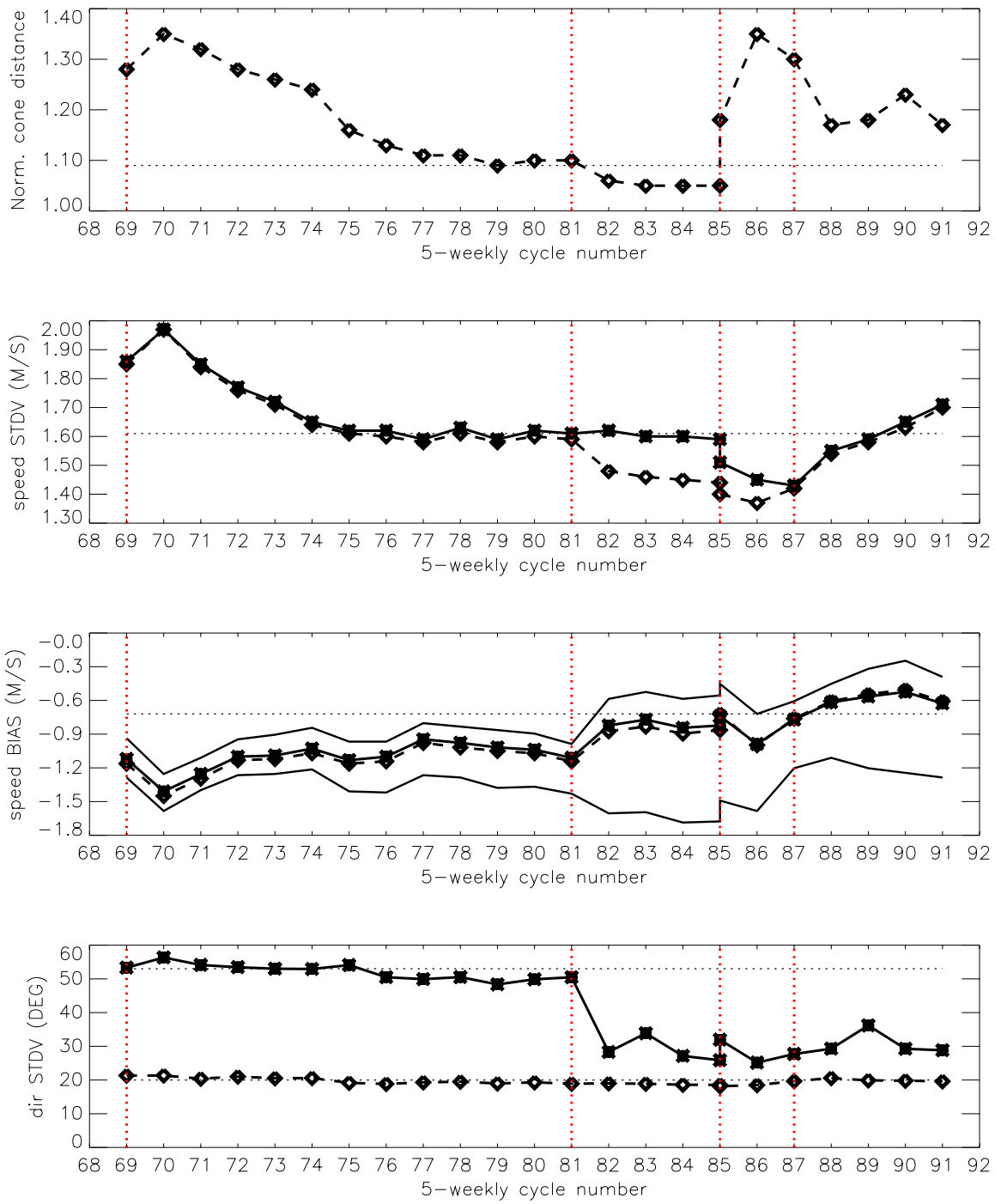
Norm. cone distance
1.40
1.30
1.20
1.10
1.00
68 69 70 71 72 73 74 75 76 77 78 79 80 81 82 83 84 85 86 87 88 89 90 91 92
5−weekly cycle number
speed STDV (M/S)
2.00
1.90
1.80
1.70
1.60
1.50
1.40
1.30
68 69 70 71 72 73 74 75 76 77 78 79 80 81 82 83 84 85 86 87 88 89 90 91 92
5−weekly cycle number
speed BIAS (M/S)
−0.0
−0.3
−0.6
−0.9
−1.2
−1.5
−1.8
68 69 70 71 72 73 74 75 76 77 78 79 80 81 82 83 84 85 86 87 88 89 90 91 92
5−weekly cycle number
dir STDV (DEG)
60
50
40
30
20
10
0
68 69 70 71 72 73 74 75 76 77 78 79 80 81 82 83 84 85 86 87 88 89 90 91 92
5−weekly cycle number

Figure 1

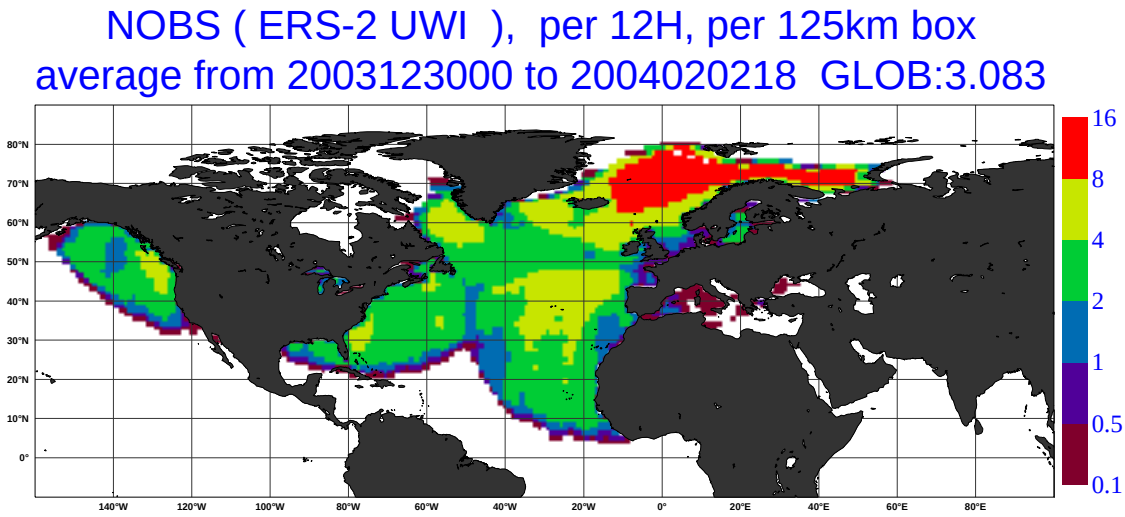
NOBS (ERS-2 UWI), per 12H, per 125km box
average from 2003123000 to 2004020218 GLOB:3.083
80°N
70°N
60°N
50°N
40°N
30°N
20°N
10°N
0°
140°W
120°W
100°W
80°W
60°W
40°W
20°W
0°
20°E
40°E
60°E
80°E
16
8
4
2
1
0.5
0.1

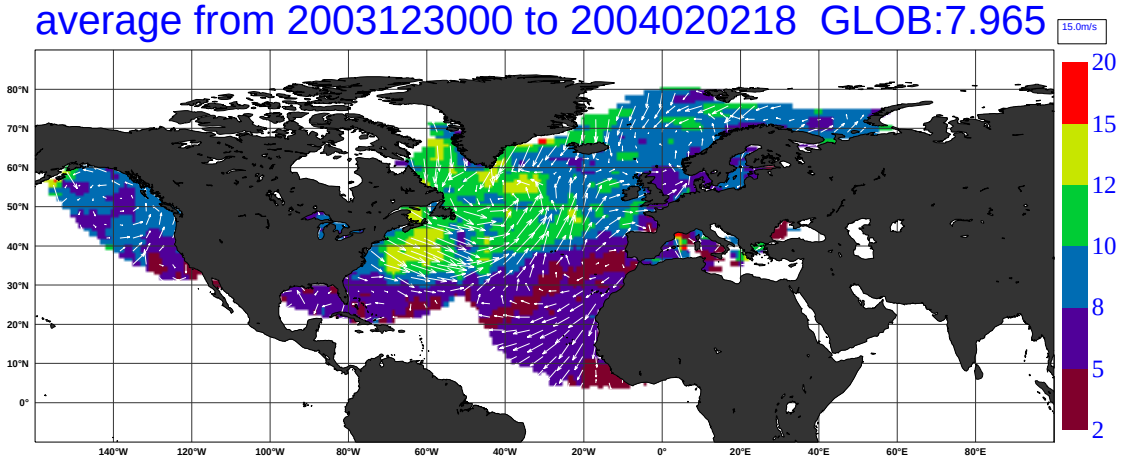
AVERAGE (ERS-2 UWI), in m/s.
average from 2003123000 to 2004020218 GLOB:7.965
15.0m/s
80°N
70°N
60°N
50°N
40°N
30°N
20°N
10°N
0°
140°W
120°W
100°W
80°W
60°W
40°W
20°W
0°
20°E
40°E
60°E
80°E
20
15
12
10
8
5
2

Figure 2

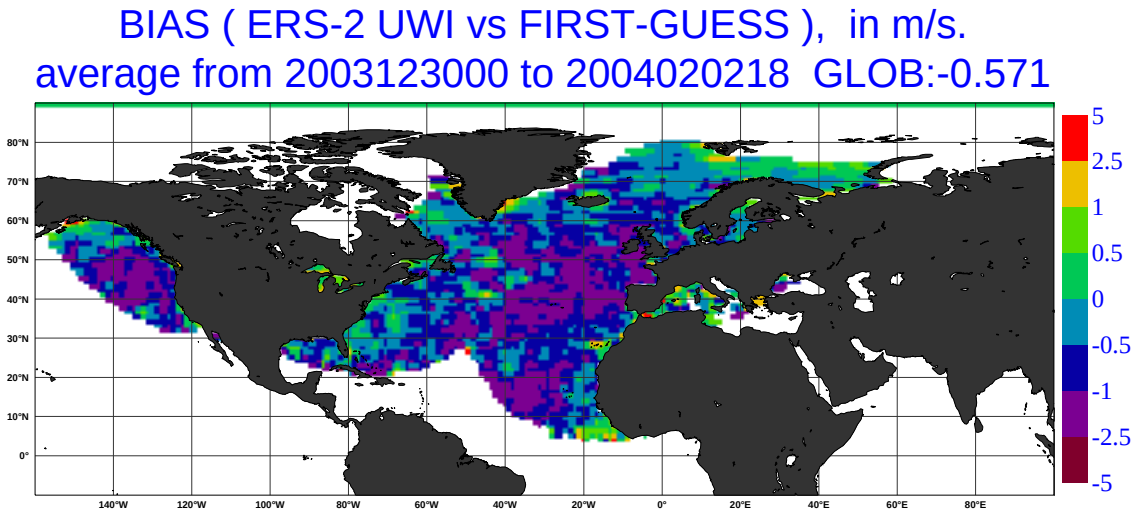
BIAS (ERS-2 UWI vs FIRST-GUESS), in m/s.
average from 2003123000 to 2004020218 GLOB:-0.571
5
2.5
1
0.5
0
-0.5
-1
-2.5
-5
80°N
70°N
60°N
50°N
40°N
30°N
20°N
10°N
0°
140°W
120°W
100°W
80°W
60°W
40°W
20°W
0°
20°E
40°E
60°E
80°E

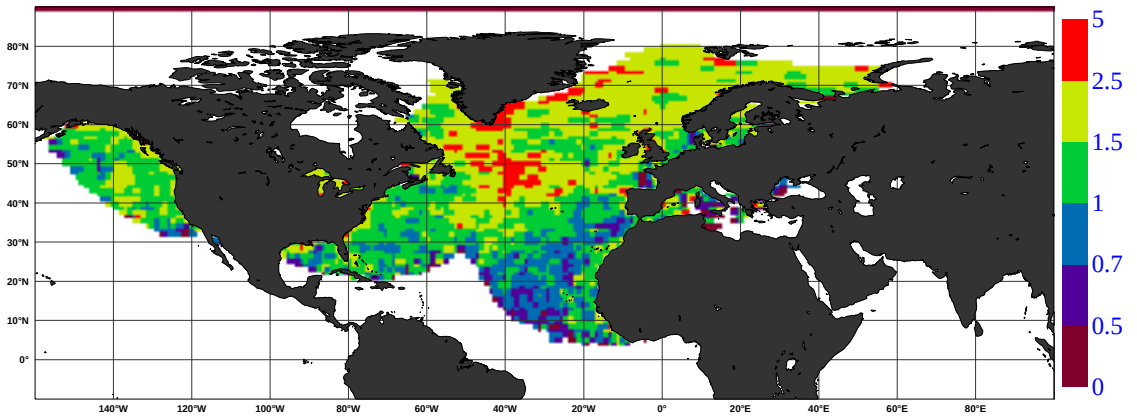
STDV (ERS-2 UWI vs FIRST-GUESS), in m/s.
average from 2003123000 to 2004020218 GLOB:1.422
5
2.5
1.5
1
0.7
0.5
0
80°N
70°N
60°N
50°N
40°N
30°N
20°N
10°N
0°
140°W
120°W
100°W
80°W
60°W
40°W
20°W
0°
20°E
40°E
60°E
80°E

Figure 3

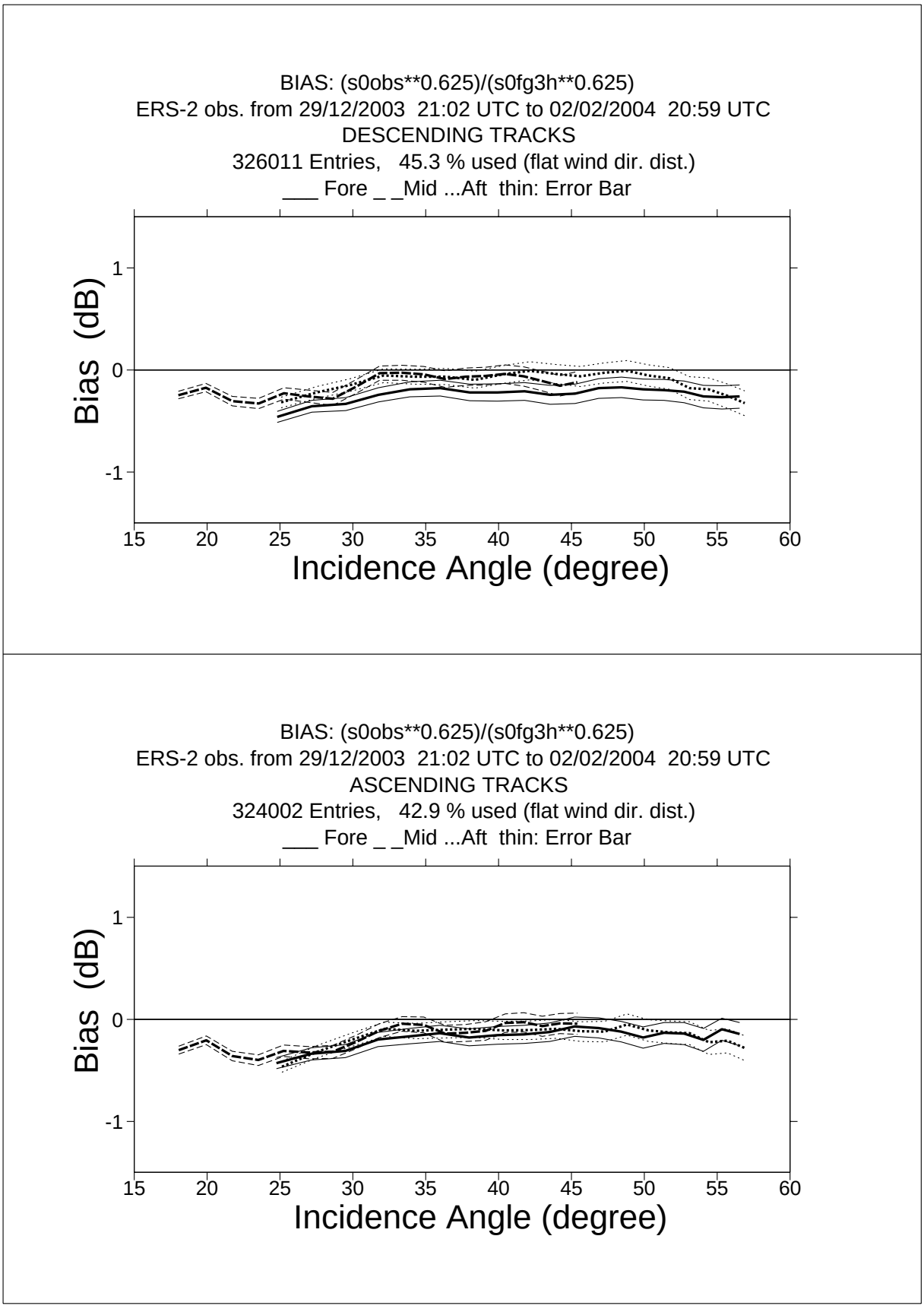
BIAS: (s0obs**0.625)/(s0fg3h**0.625)
ERS-2 obs. from 29/12/2003 21:02 UTC to 02/02/2004 20:59 UTC
DESCENDING TRACKS
326011 Entries, 45.3 % used (flat wind dir. dist.)
___ Fore _ _Mid ...Aft thin: Error Bar
Bias (dB)
1
0
-1
15
20
25
30
35
40
45
50
55
60
Incidence Angle (degree)
BIAS: (s0obs**0.625)/(s0fg3h**0.625)
ERS-2 obs. from 29/12/2003 21:02 UTC to 02/02/2004 20:59 UTC
ASCENDING TRACKS
324002 Entries, 42.9 % used (flat wind dir. dist.)
___ Fore _ _Mid ...Aft thin: Error Bar
Bias (dB)
1
0
-1
15
20
25
30
35
40
45
50
55
60
Incidence Angle (degree)

Figure 4

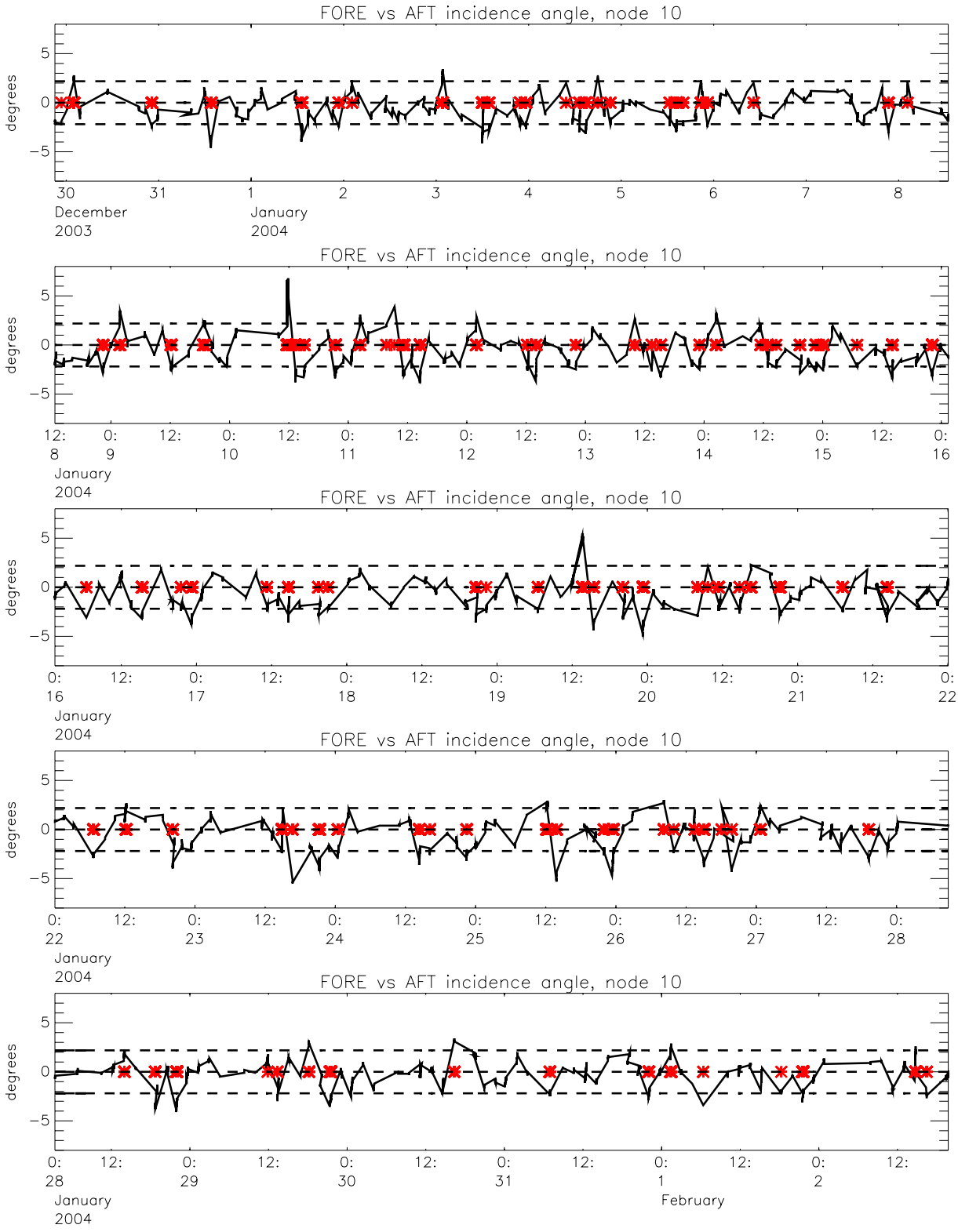
FORE vs AFT incidence angle, node 10
degrees
5
0
−5
30 31 1 2 3 4 5 6 7 8
December 2003
January 2004
FORE vs AFT incidence angle, node 10
degrees
5
0
−5
12: 0: 12: 0: 12: 0: 12: 0: 12: 0: 12: 0: 12: 0: 12: 0:
8 9 10 11 12 13 14 15 16
January 2004
FORE vs AFT incidence angle, node 10
degrees
5
0
−5
0: 12: 0: 12: 0: 12: 0: 12: 0: 12: 0: 12: 0:
16 17 18 19 20 21 22
January 2004
FORE vs AFT incidence angle, node 10
degrees
5
0
−5
0: 12: 0: 12: 0: 12: 0: 12: 0: 12: 0: 12: 0:
22 23 24 25 26 27 28
January 2004
FORE vs AFT incidence angle, node 10
degrees
5
0
−5
0: 12: 0: 12: 0: 12: 0: 12: 0: 12: 0: 12:
28 29 30 31 1 2
January 2004
February

Figure 5

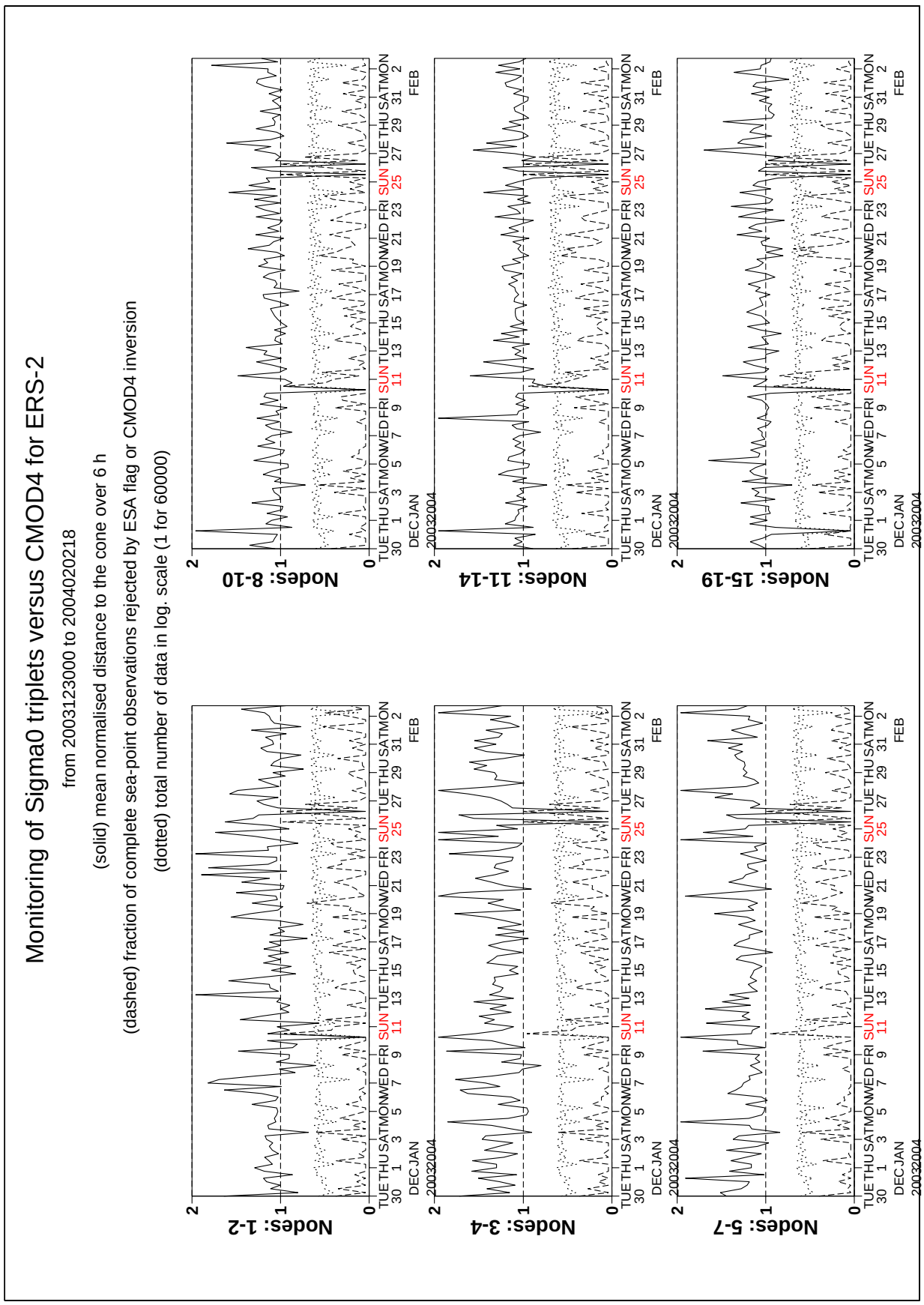
Monitoring of Sigma0 triplets versus CMOD4 for ERS-2
from 2003123000 to 2004020218
(solid) mean normalised distance to the cone over 6 h
(dashed) fraction of complete sea-point observations rejected by ESA flag or CMOD4 inversion
(dotted) total number of data in log. scale (1 for 60000)
Nodes: 1-2
Nodes: 3-4
Nodes: 5-7
Nodes: 8-10
Nodes: 11-14
Nodes: 15-19
TUE THU SAT MON WED FRI SUN TUE THU SAT MON WED FRI SUN TUE THU SAT MON
30 1 3 5 7 9 11 13 15 17 19 21 23 25 27 29 31 2
DEC JAN FEB
2003 2004

Figure 6

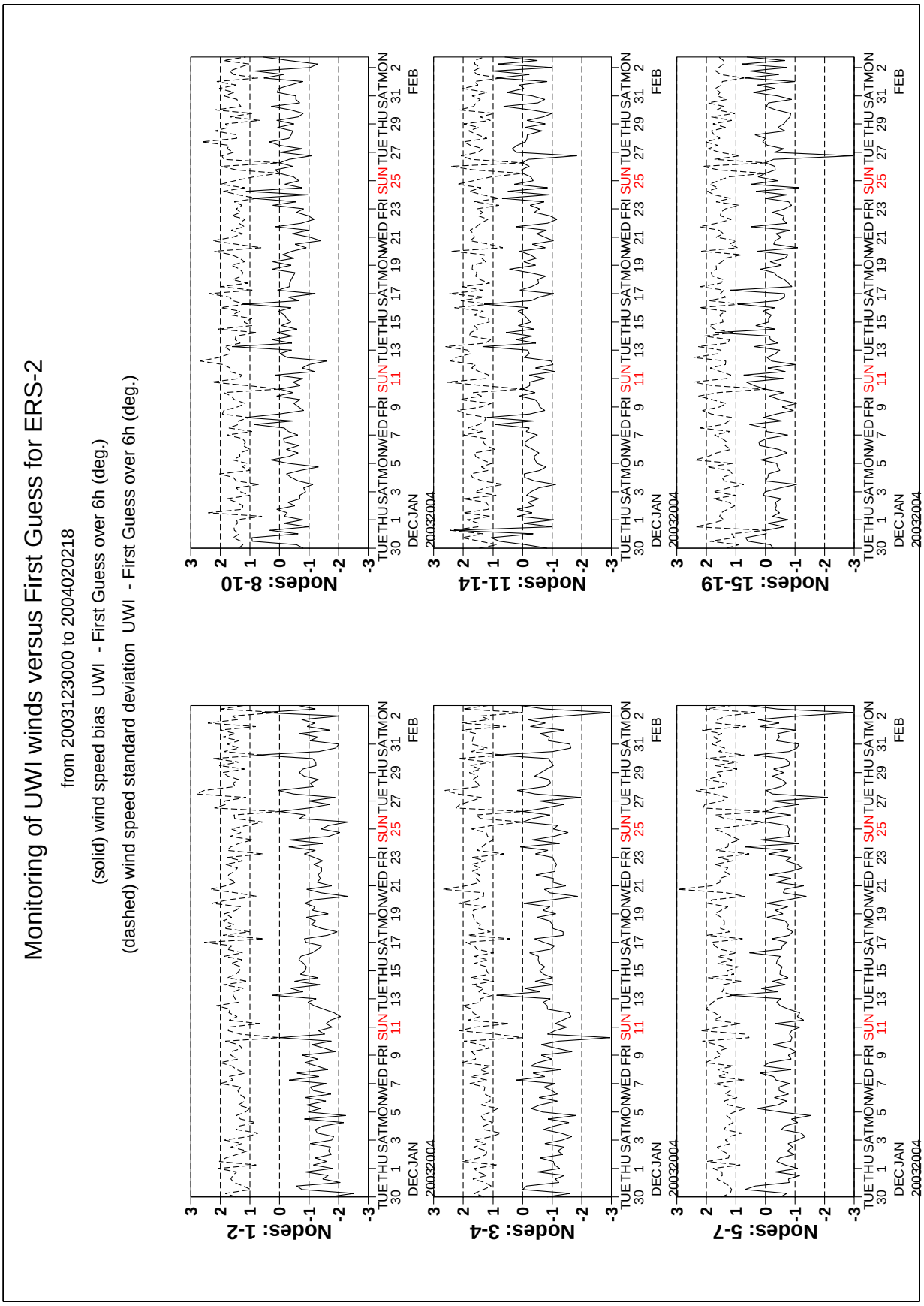
Monitoring of UWI winds versus First Guess for ERS-2
from 2003123000 to 2004020218
(solid) wind speed bias UWI - First Guess over 6h (deg.)
(dashed) wind speed standard deviation UWI - First Guess over 6h (deg.)
Nodes: 1-2
Nodes: 3-4
Nodes: 5-7
Nodes: 8-10
Nodes: 11-14
Nodes: 15-19
DEC JAN FEB
2003 2004

Figure 7

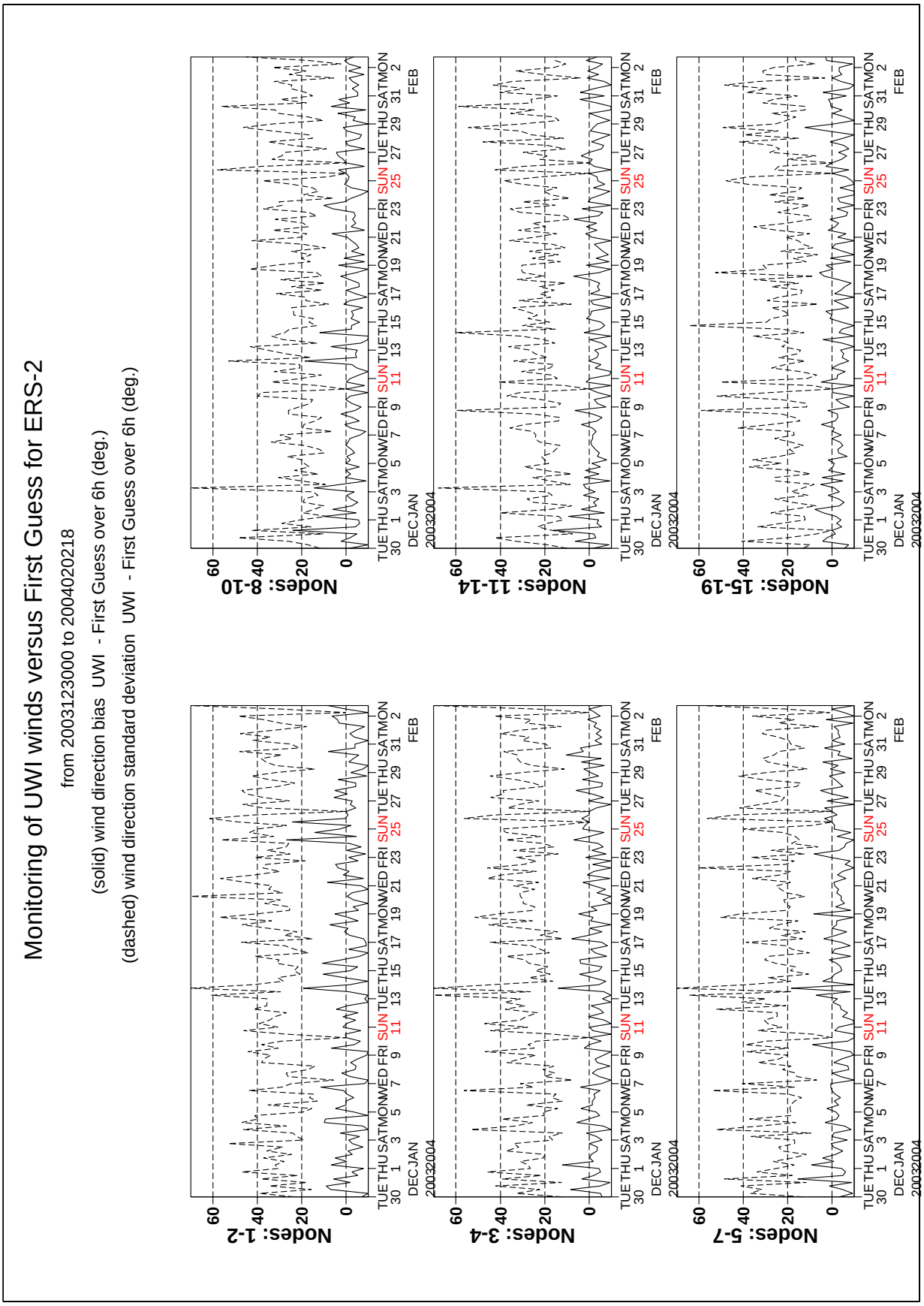
Monitoring of UWI winds versus First Guess for ERS-2
from 2003123000 to 2004020218
(solid) wind direction bias UWI - First Guess over 6h (deg.)
(dashed) wind direction standard deviation UWI - First Guess over 6h (deg.)
Nodes: 1-2
Nodes: 3-4
Nodes: 5-7
Nodes: 8-10
Nodes: 11-14
Nodes: 15-19
TUE THU SAT MON WED FRI SUN TUE THU SAT MON WED FRI SUN TUE THU SAT MON
30 1 3 5 7 9 11 13 15 17 19 21 23 25 27 29 31 2
DEC JAN FEB
2003 2004
0 20 40 60

Figure 8

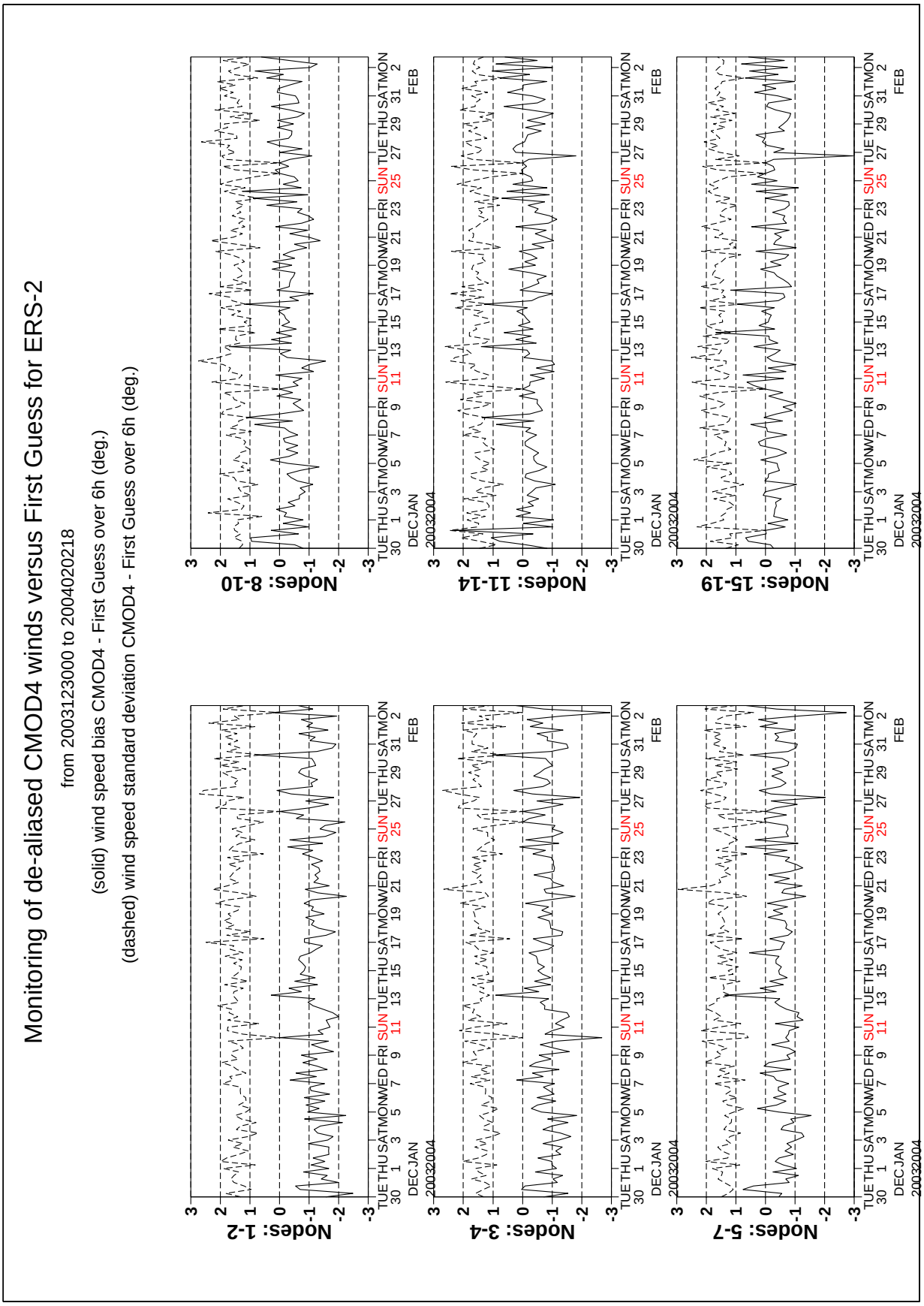
Monitoring of de-aliased CMOD4 winds versus First Guess for ERS-2
from 2003123000 to 2004020218
(solid) wind speed bias CMOD4 - First Guess over 6h (deg.)
(dashed) wind speed standard deviation CMOD4 - First Guess over 6h (deg.)
Nodes: 1-2
Nodes: 3-4
Nodes: 5-7
Nodes: 8-10
Nodes: 11-14
Nodes: 15-19
TUE THU SAT MON WED FRI SUN TUE THU SAT MON WED FRI SUN TUE THU SAT MON
30 1 3 5 7 9 11 13 15 17 19 21 23 25 27 29 31 2
DEC JAN FEB
20032004

Figure 9

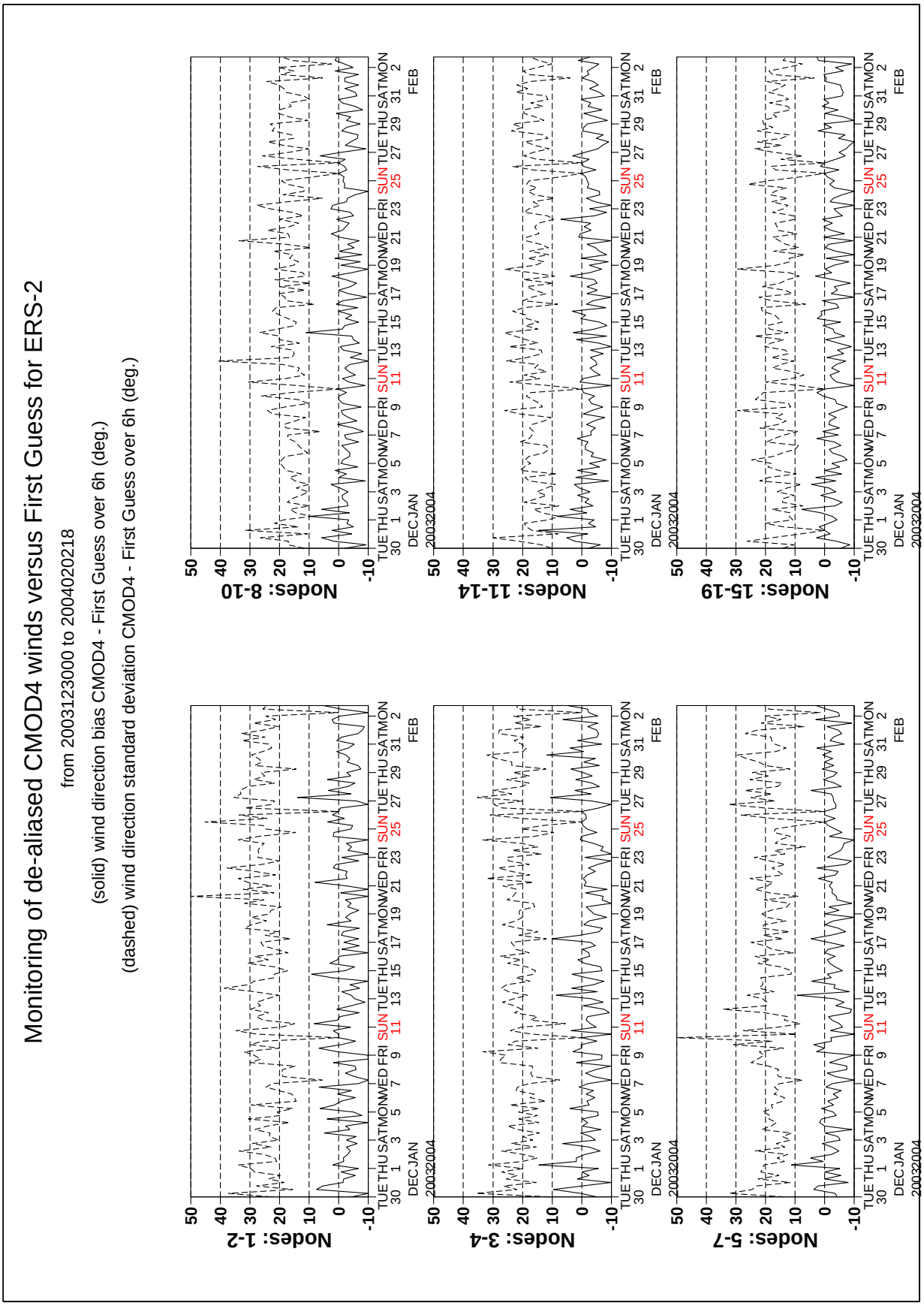
Monitoring of de-aliased CMOD4 winds versus First Guess for ERS-2
from 2003123000 to 2004020218
(solid) wind direction bias CMOD4 - First Guess over 6h (deg.)
(dashed) wind direction standard deviation CMOD4 - First Guess over 6h (deg.)
Nodes: 1-2
Nodes: 3-4
Nodes: 5-7
Nodes: 8-10
Nodes: 11-14
Nodes: 15-19
50
40
30
20
10
0
-10
TUE THU SAT MON WED FRI SUN TUE THU SAT MON WED FRI SUN TUE THU SAT MON
30 1 3 5 7 9 11 13 15 17 19 21 23 25 27 29 31 2
DEC JAN FEB
20032004

Figure 10

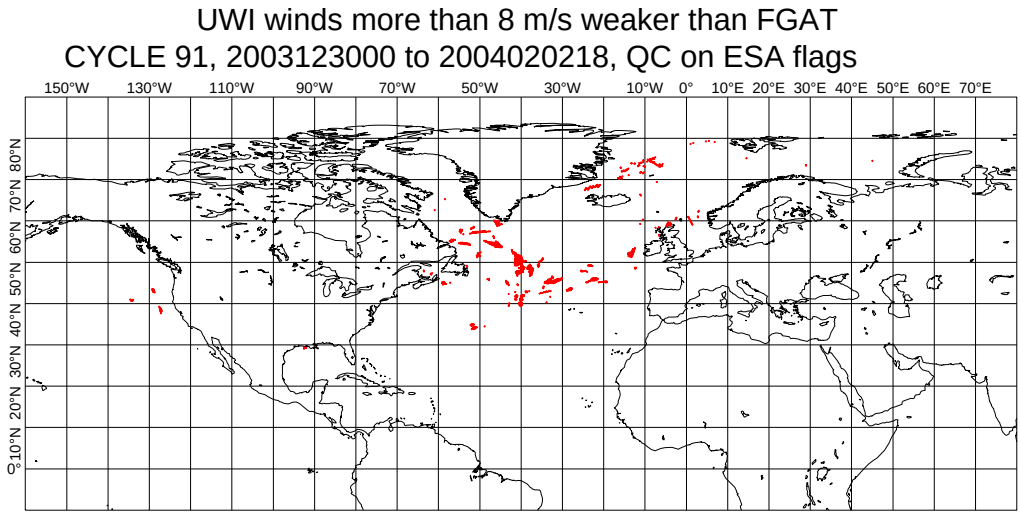
UWI winds more than 8 m/s weaker than FGAT
CYCLE 91, 2003123000 to 2004020218, QC on ESA flags
150°W 130°W 110°W 90°W 70°W 50°W 30°W 10°W 0° 10°E 20°E 30°E 40°E 50°E 60°E 70°E
80°N 70°N 60°N 50°N 40°N 30°N 20°N 10°N 0°

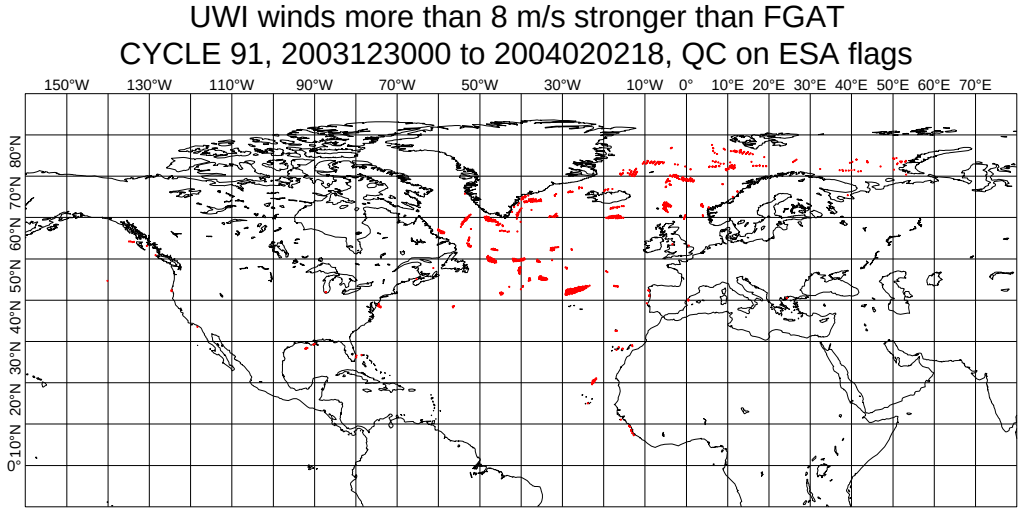
UWI winds more than 8 m/s stronger than FGAT
CYCLE 91, 2003123000 to 2004020218, QC on ESA flags
150°W 130°W 110°W 90°W 70°W 50°W 30°W 10°W 0° 10°E 20°E 30°E 40°E 50°E 60°E 70°E
80°N 70°N 60°N 50°N 40°N 30°N 20°N 10°N 0°

Figure 11

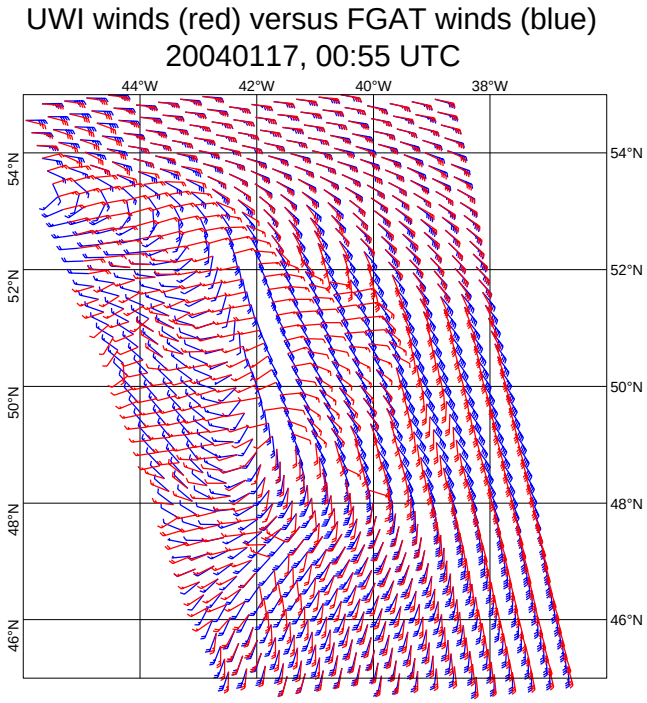
UWI winds (red) versus FGAT winds (blue)
20040117, 00:55 UTC
44°W
42°W
40°W
38°W
54°N
52°N
50°N
48°N
46°N

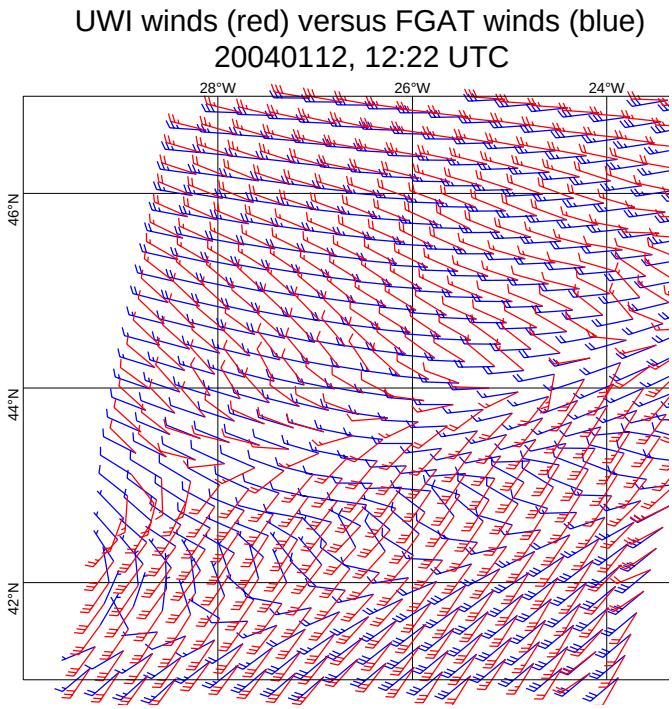
UWI winds (red) versus FGAT winds (blue)
20040112, 12:22 UTC
28°W
26°W
24°W
46°N
44°N
42°N

Figure 12

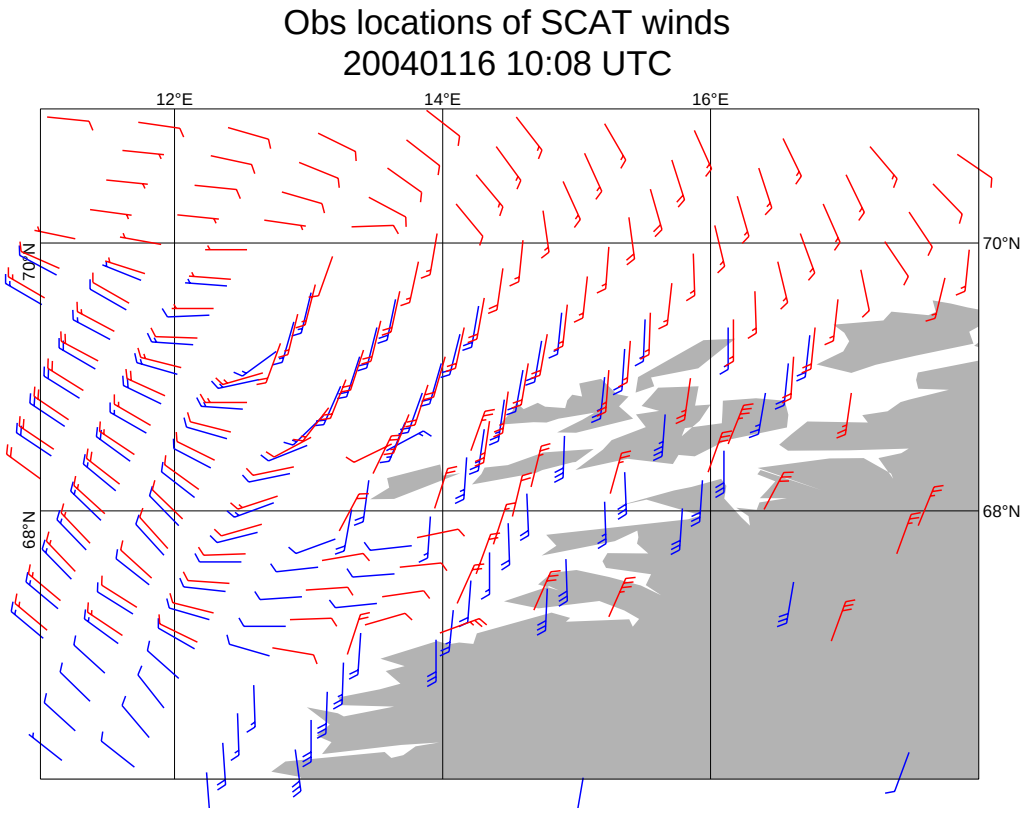
Obs locations of SCAT winds
20040116 10:08 UTC
12°E
14°E
16°E
70°N
68°N

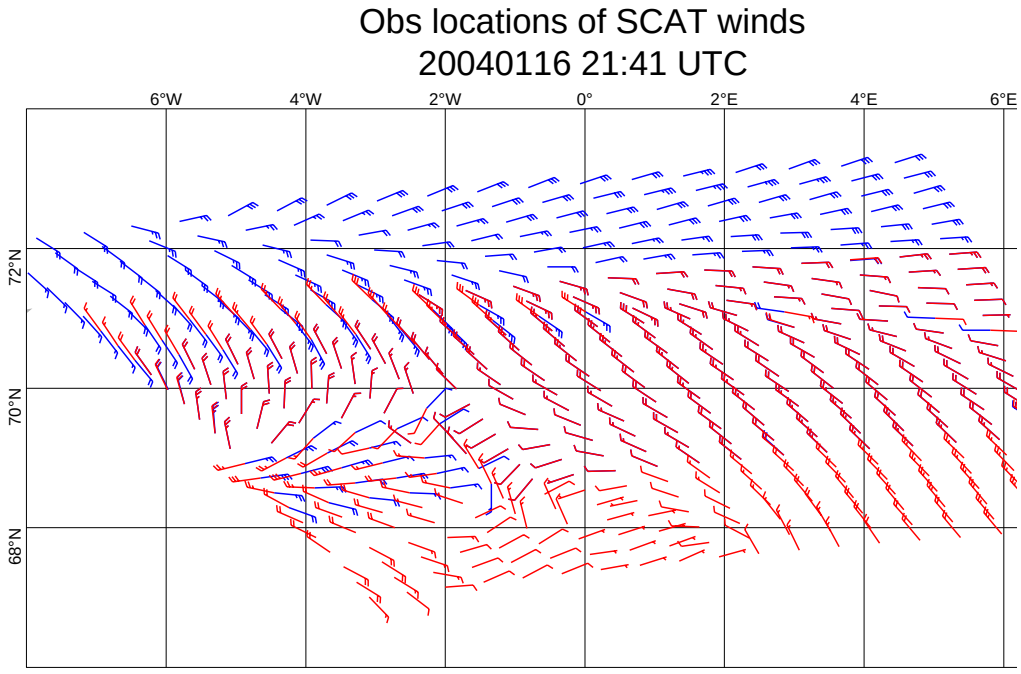
Obs locations of SCAT winds
20040116 21:41 UTC
6°W
4°W
2°W
0°
2°E
4°E
6°E
72°N
70°N
68°N

Figure 13

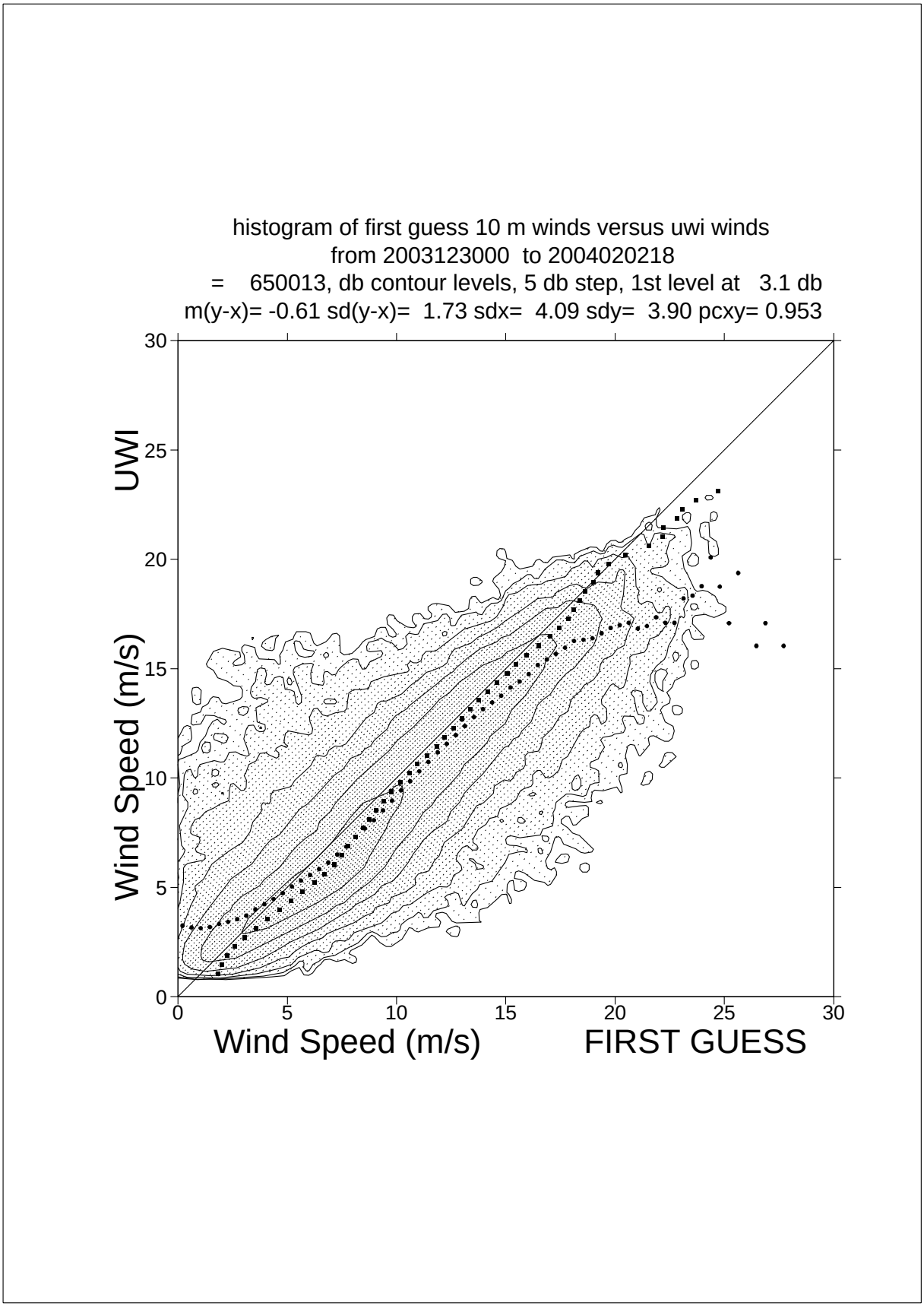
histogram of first guess 10 m winds versus uwi winds
from 2003123000 to 2004020218
= 650013, db contour levels, 5 db step, 1st level at 3.1 db
m(y-x)= -0.61 sd(y-x)= 1.73 sdx= 4.09 sdy= 3.90 pcxy= 0.953
UWI
Wind Speed (m/s)
0
5
10
15
20
25
30
Wind Speed (m/s)
FIRST GUESS

Figure 14

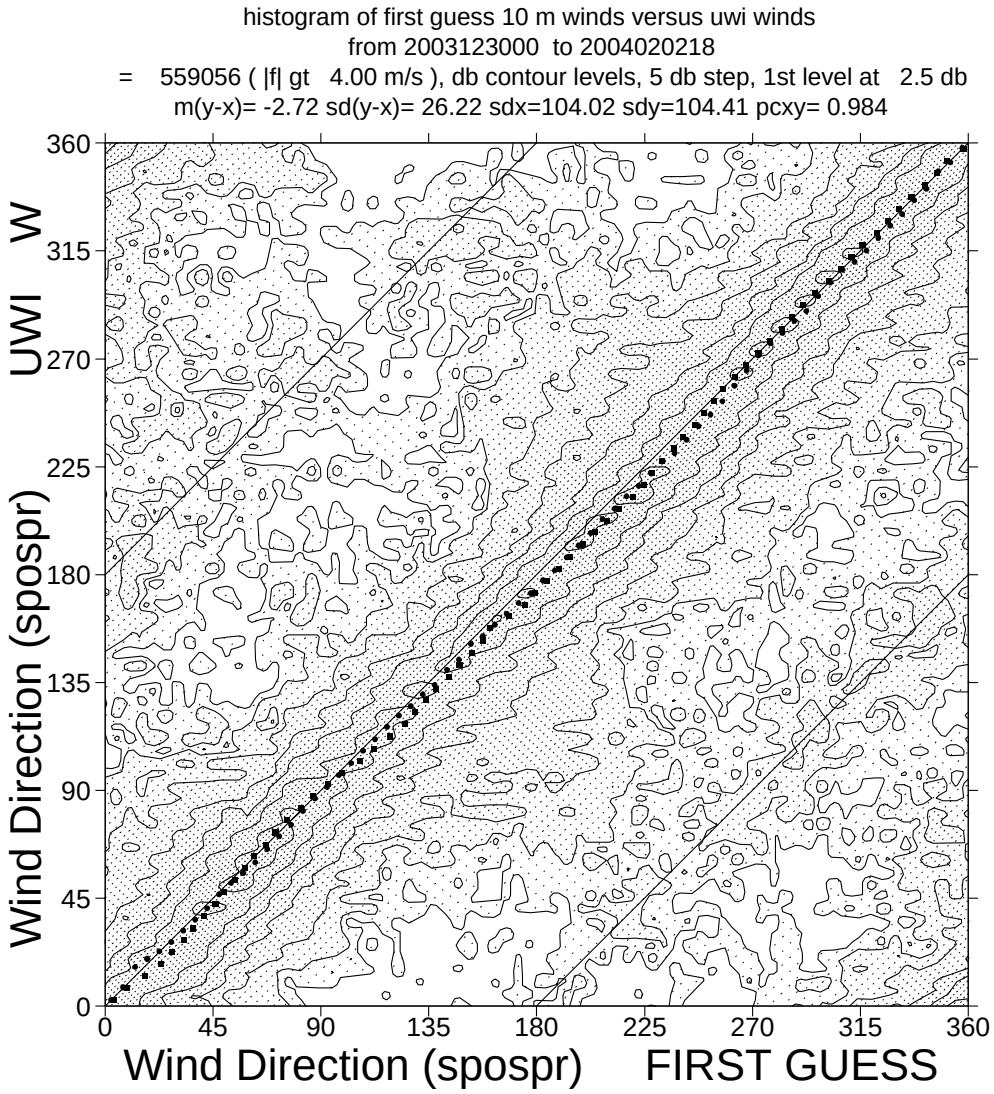
histogram of first guess 10 m winds versus uwi winds
from 2003123000 to 2004020218
= 559056 (|f| gt 4.00 m/s), db contour levels, 5 db step, 1st level at 2.5 db
m(y-x)= -2.72 sd(y-x)= 26.22 sdx=104.02 sdy=104.41 pcxy= 0.984
UWI W
Wind Direction (spospr)
0
45
90
135
180
225
270
315
360
Wind Direction (spospr) FIRST GUESS

Figure 15

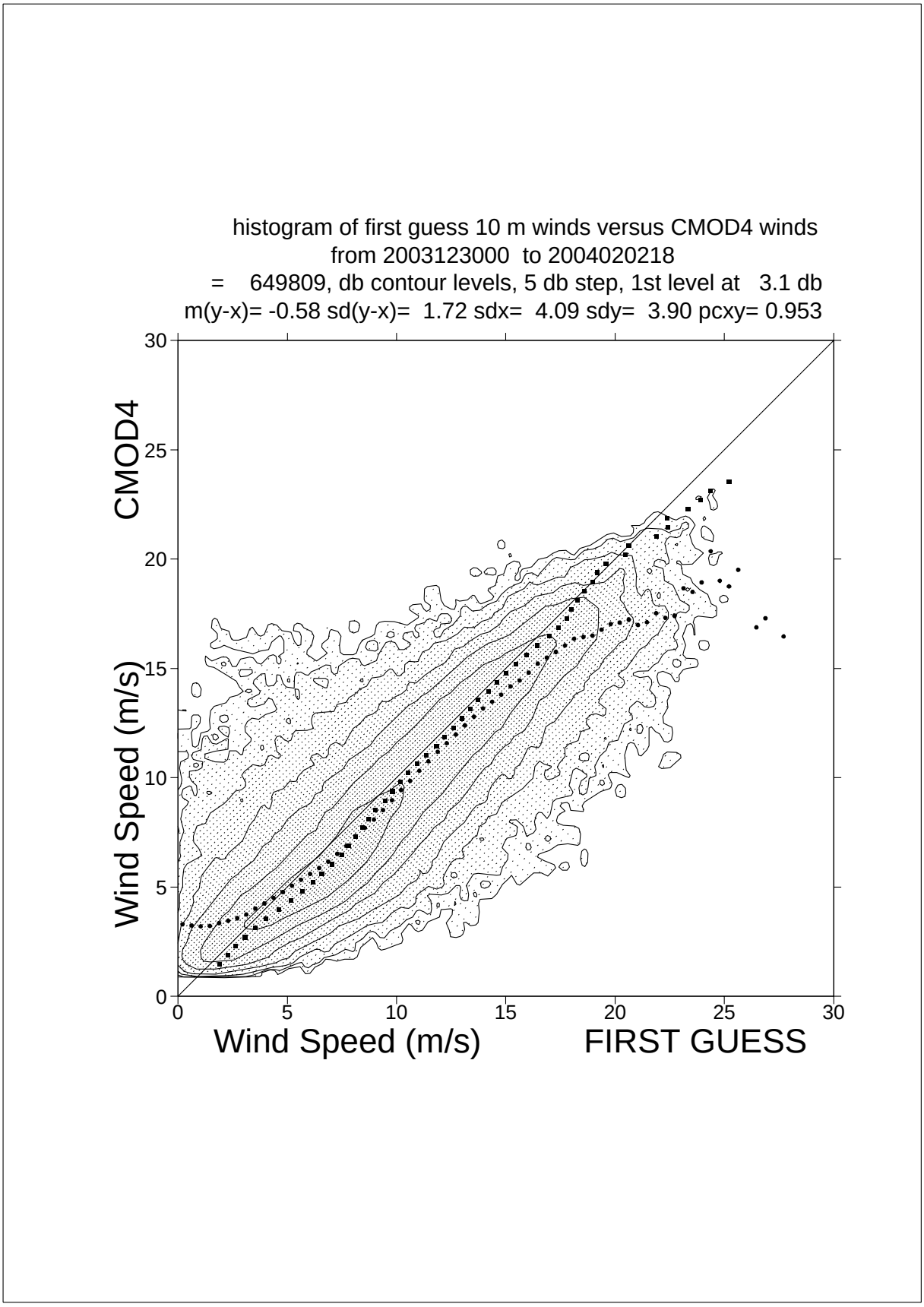
histogram of first guess 10 m winds versus CMOD4 winds
from 2003123000 to 2004020218
= 649809, db contour levels, 5 db step, 1st level at 3.1 db
m(y-x)= -0.58 sd(y-x)= 1.72 sdx= 4.09 sdy= 3.90 pcxy= 0.953
CMOD4
Wind Speed (m/s)
0
5
10
15
20
25
30
Wind Speed (m/s)
FIRST GUESS

Figure 16

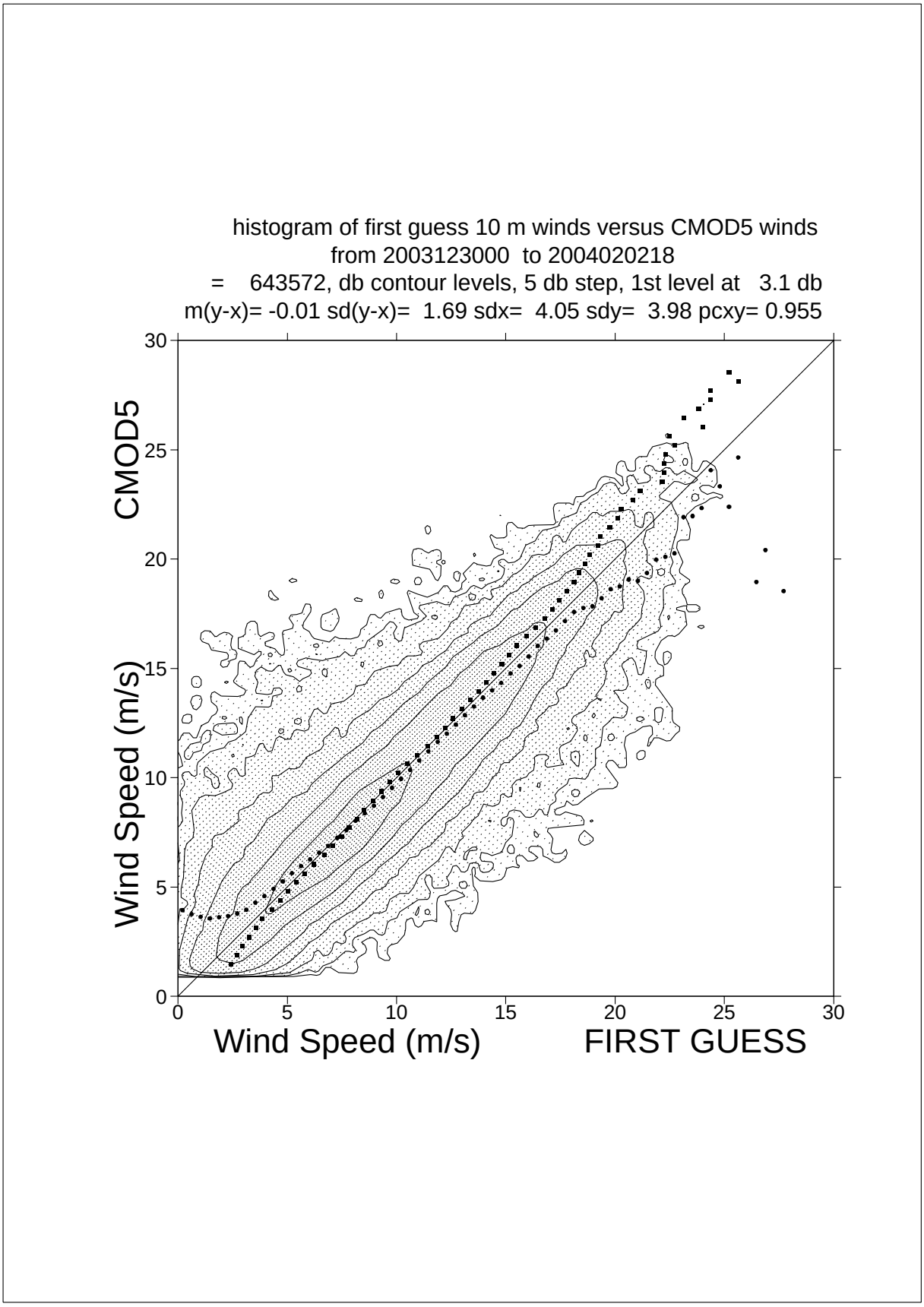
histogram of first guess 10 m winds versus CMOD5 winds
from 2003123000 to 2004020218
= 643572, db contour levels, 5 db step, 1st level at 3.1 db
m(y-x)= -0.01 sd(y-x)= 1.69 sdx= 4.05 sdy= 3.98 pcxy= 0.955
CMOD5
Wind Speed (m/s)
0
5
10
15
20
25
30
Wind Speed (m/s)
FIRST GUESS

Figure 17